SUPPORTING INFORMATION FOR

Brominated Tyrosine and Polyelectrolyte Multilayer Analysis by Laser Desorption VUV Postionization and Secondary Ion Mass Spectrometry

Melvin Blaze M.T.[1], Lynelle K. Takahashi[2,3], Jia Zhou[3], Musahid Ahmed[3], F. Douglas Pleticha[1], and Luke Hanley[1,*]

[1]Department of Chemistry, University of Illinois at Chicago, Chicago, IL 60607
[2]Department of Chemistry, University of California, Berkeley, Berkeley, CA 94720
[3]Chemical Sciences Division, Lawrence Berkeley National Laboratory, Berkeley, CA 94720

S1. Preparation of PEMs. Polyelectrolyte multilayers (PEMs) with 10 alternating layers each of chitosan and alginate were prepared on gold-coated silicon substrates using cysteamine and glutaraldehyde as linkers by dip coating as shown in Figures S1 and S2.

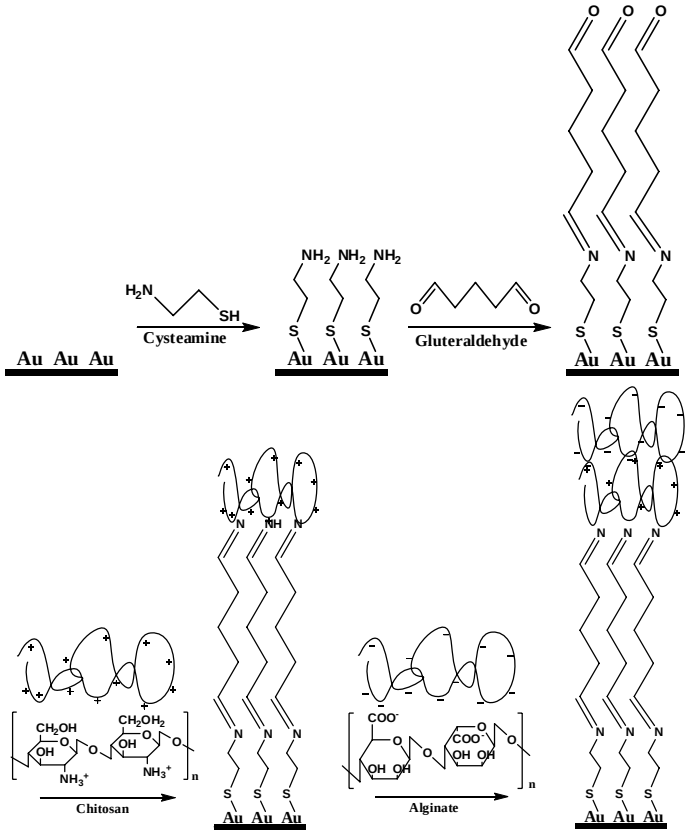

Figure S1. Preparation of polyelectrolyte multilayers (PEMs), up to first dual layer of chitosan and alginate.

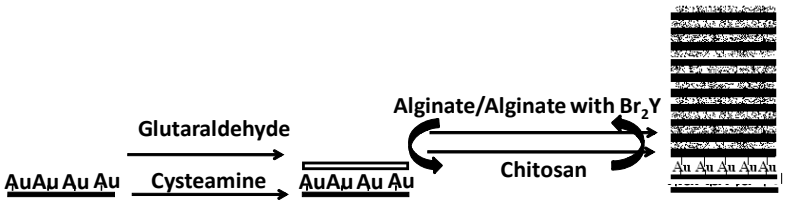

Figure S2. Preparation of PEMs consisting of a total of ten layers each of chitosan and alginate, some with 2,5-dibromotyrosine (Br_2Y) adsorbed into every alternating alginate layer (Br_2Y-PEMs).

PEM2 were prepared by a method described previously.[15,17] The Au substrate was first cleaned by sonication in piranha solution consisting of (7:3 v:v) concentrated sulfuric acid:30% hydrogen peroxide, then rinsed several times with distilled water. A cysteamine solution was used to prepare a self-assembled monolayer on the gold surface, which was then reacted with a glutaraldehyde solution that covalently bound the first polysaccharide layer of chitosan. The modified substrate was then manually immersed alternately in chitosan solution (0.2% w:v dissolved in 2% v:v acetic acid solution) and sodium alginate (2% w:v in water) for one hour each, with intermediate rinsing using deionized water. The resultant PEMs consisted of a total of ten alternating layers each of chitosan and alginate. Br_2Y was incorporated in every alternating layer of PEM as a zwitterion mixed with the unmodified alginate solution to form the Br_2Y-PEM (see Figure S2).

S2. Verification of PEMs. PEMs were verified by attenuated total reflection Fourier transform infrared spectroscopy (ATR-FTIR). ATR-FTIR spectra were acquired (ABB FTLA2000 spectrometer) with a germanium ATR crystal by collecting 120 scans at 2 cm^{-1} resolution with a wavenumber range of 4600 - 500 cm^{-1}. Background spectra were recorded using a gold-coated substrate cleaned with piranha solution. Spectral manipulations were performed using commercial analysis software (GRAMS/32). Figure S3 shows the ATR-FTIR spectra for a PEM with single alternating layers of chitosan and alginate which displays peaks characteristic to chitosan and alginate. Figure S4 shows the ATR-FTIR spectra for PEMs with

two, five, and fifteen layers: more layers show higher intensity of peaks characteristic to chitosan and alginate, confirming the formation of PEMs.

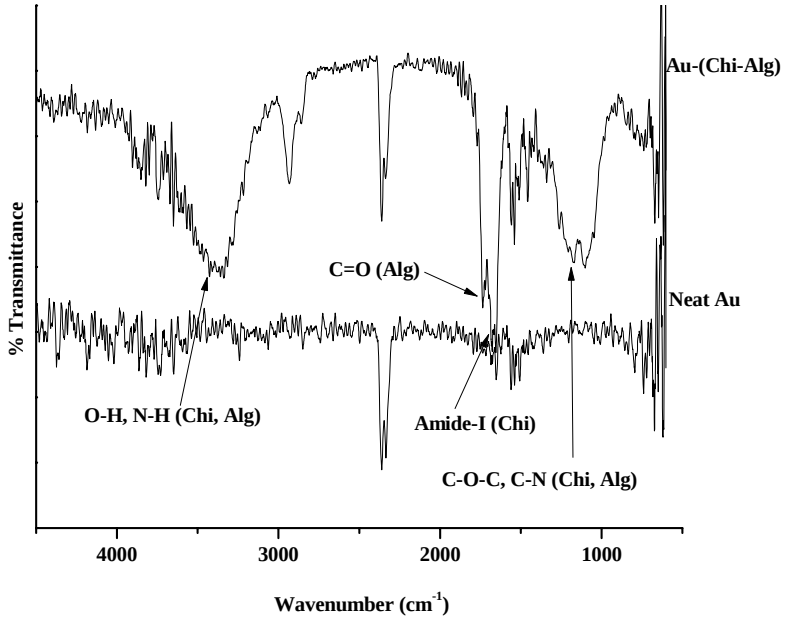

Figure S3. ATR-FTIR spectra showing alginate and chitosan characteristic peaks from (top) single alternating layers of alginate and chitosan on Au. Also shown (bottom) is the ATR-FTIR of a clean Au substrate.

The fully prepared PEMs were also analyzed by monochromatic X-ray photoelectron spectroscopy using instrumentation and procedures previously described.[18] Elemental content was determined by peak fitting the carbon *1s*, nitrogen *1s*, oxygen *1s* and bromine $3d_{5/2}$ core level X-ray photoelectron spectra using commercial software (XPS Peak 4.1) after correcting for elemental dependences on photoionization cross section.

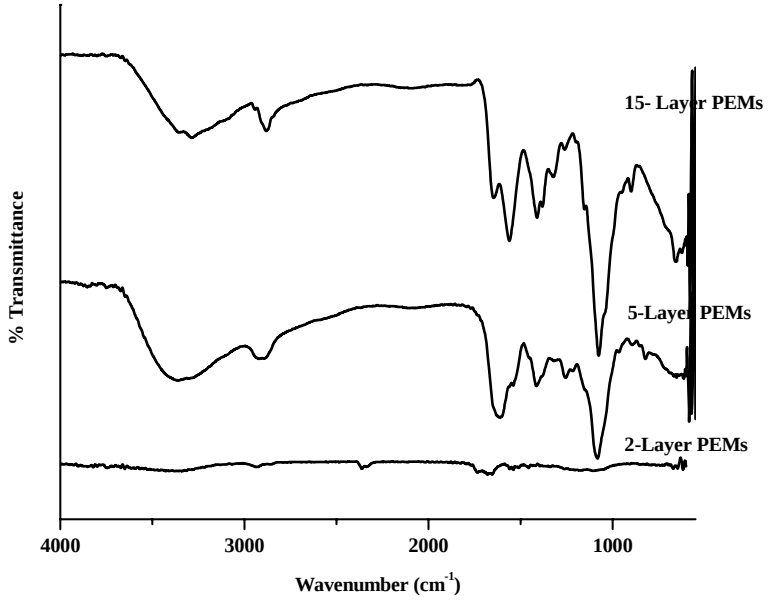

Figure S4. ATR-FTIR spectra of PEMs of two, five, and fifteen layers.

S3. 8 – 12.5 eV Synchrotron LDPI-MS and SIMS. Synchrotron LDPI-MS and SIMS were recorded using a commercial SIMS instrument (TOF.SIMS 5, ION-TOF Inc., Munster, Germany) equipped with a bismuth liquid metal ion gun emitting 25 keV Bi_3^+ pulses at 10 kHz.[8] The SIMS instrument was modified for LDPI-MS by the addition of a 349 nm pulsed desorption laser (Explorer, Newport) operating at 2500 Hz with a spot size of ~30 μm diameter and typical laser desorption peak power density of 1 to 10 MW/cm^2. The laser desorbed neutral molecules were photoionized by 8.0 to 12.5 eV tunable VUV synchrotron radiation from the Chemical Dynamics Beamline at the Advanced Light Source (Lawrence Berkeley National Laboratory, Berkeley, CA)[16] The photoionized neutrals were extracted using a 5 μs extraction pulse with a delay time of 1.2 – 1.4 μs with respect to the desorption pulse. 143,000 laser shots on a single spot were used for each displayed mass spectrum.

This instrument was also used to record photoionization efficiency curves of gas phase Br_2Y molecules by thermally heating the sample above 120°C while scanning the VUV photon energy, without any ion or laser desorption.

S4. 7.87 eV Laser LDPI-MS. 7.87 eV laser LDPI-MS was collected using a custom built instrument at the University of Illinois at Chicago which is equipped with a 157.6 nm pulsed laser for photoionization and was described in detail previously.[6] This LDPI-MS has a 349 nm Nd:YLF desorption laser operating at 100 Hz, with a spot size of ~20 μm diameter and typical desorption laser peak power density ranging from 30 to 70 MW/cm^2. The sample was rastered at 100 μm/s with respect to the laser, so each 20 μm sample spot was sampled by ~20 desorption laser shots and a total of 50 – 100 laser shots were sufficient to obtain spectra with optimal signal to noise. The desorbed neutral molecules were photoionized using a 157.6 nm (7.87 eV) molecular fluorine excimer laser operating at a 100 Hz with a spot size of approximately 8 mm in the ionization region and an energy of ~100 μJ/pulse. The photoionized neutrals were extracted using a pseudo-orthogonal delayed pulsed extraction and detected by a home-built two-stage reflectron time of flight mass spectrometer. Spectra were recorded at a delay of 3.9 μs between the photoionization laser and the extraction pulse. Varying this delay by a few μs affected the absolute signal, but not the overall appearance of the spectra. The instrument was also equipped with an ultrahigh vacuum compatible translation stage for sample manipulation and a digital single lens reflex camera for real time sample viewing on a high definition television. Data acquisition and sample stage movements were computer controlled using customized software.

S5. Single Photon Ionization (SPI) MS of Evaporated Br_2Y. The data in Figure S5 displays the relative $[Br_2Y]^+$ parent ion signal from evaporated Br_2Y as a function of photon energy as a function of synchrotron photon energies. Full SPI-MS were recorded at each photon energy point on the curve in Figure S5 and two of these spectra, recorded at 9.45 and 11.5 eV photon energies, are shown in Figure S6. 9.45 eV corresponds to ~1.1 eV internal energy deposited into the parent ion (the photon energy minus the ionization energy) while 11.5 eV corresponds to ~3.2 eV internal energy in the parent ion. The increase in internal energy significantly enhanced fragmentation in the parent ion at the higher photon energy, as expected.

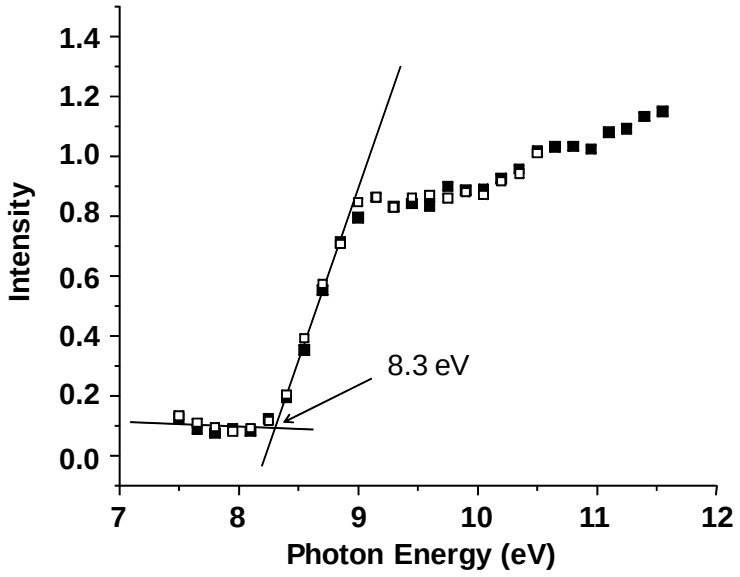

Figure S5. Photoionization efficiency curve for Br_2Y thermally desorbed from pure films recorded by sweeping the VUV photon energy while monitoring the m/z 337 parent ion. Intensities normalized to data collected at 10.5 eV photon energy. Lines are extrapolations indicating 8.3±0.1 eV experimental ionization energy. The different symbols correspond to different runs.

Several of the fragments observed in SPI-MS of evaporated Br_2Y are similar to those from LDPI-MS of Br_2Y films (see Figure 1). Specifically, the II, III, and V fragments identified in Figure 2 were observed along with the parent ion by SPI-MS and ≤8.0 eV LDPI-MS. However, little to none of the I, V, and VI fragments observed by LDPI-MS were detected by

SPI-MS. Furthermore, SPI-MS additionally detected a deprotonated III fragment ion, denoted as $[III-H]^+$ in Figure S6, which was not observed at all in LDPI-MS. There were also significant differences in the fragment/parent ion ratios between LDPI-MS and SPI-MS: the (II/parent) and (III/parent) ratios were much higher in LDPI-MS than in SPI-MS, indicating a greater extent of fragmentation in the former and differences in fragmentation mechanisms between the two cases. Finally, there were no cluster ions observed by SPI-MS, unlike the case for LDPI-MS (Figure 3).

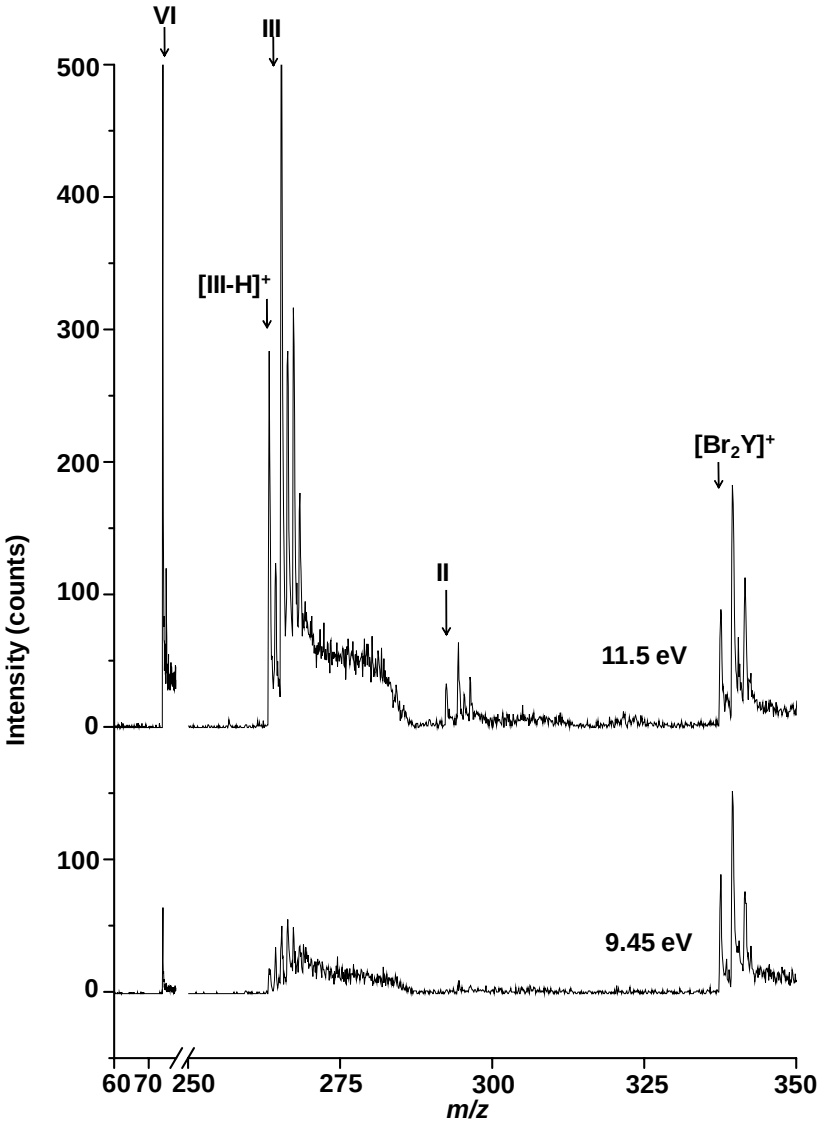

Figure S6. 9.45 and 11.5 eV photon energy SPI-MS of Br_2Y using synchrotron radiation.

S6. Geometries Used for Electronic Structure Calculation of Ionization Energies. Ionization energies (IEs) of Br_2Y , $[Br_2Y]_2$, [Br2Y][H2O] and $[Br2Y][H2O]_3$ were calculated using density functional theory in Gaussian 03.[19] The optimized geometries in the ground state shown in Figures S7 – S10 were used to calculate the vertical IEs by freezing the geometries and removing one electron from the highest occupied molecular orbital All calculations were performed at the B3LYP/6-311+G** level and were corrected for zero point energy on the structures shown in the Supporting Information that represented local minima on their respective potential energy surfaces.

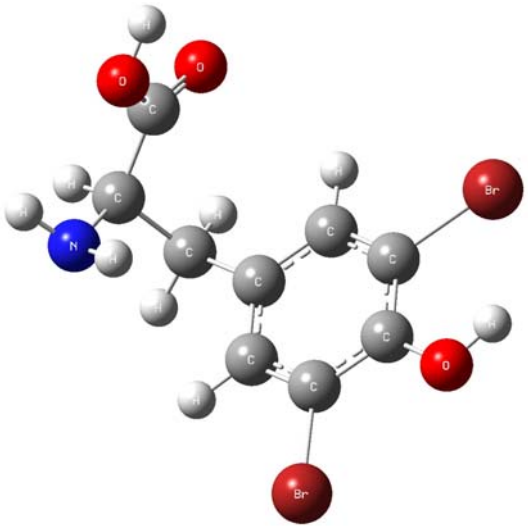

Figure S7. Optimized geometry of Br_2Y.

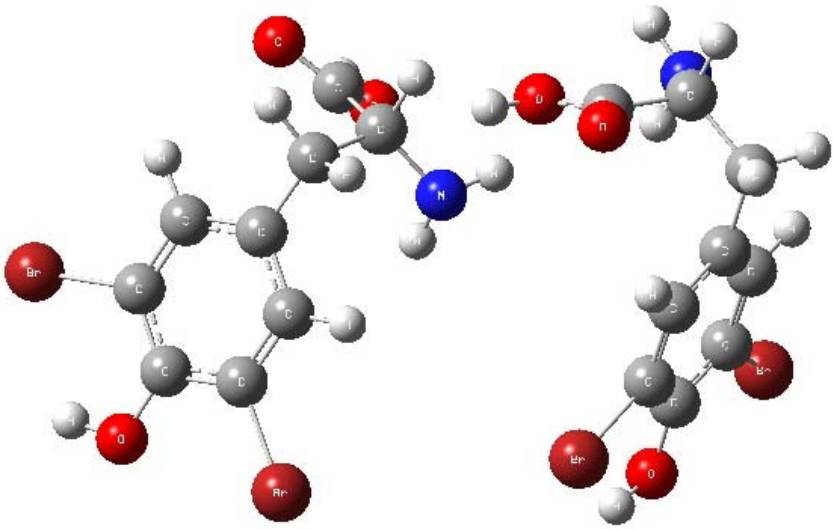

Figure S8. Optimized geometry of $[Br_2Y]_2$.

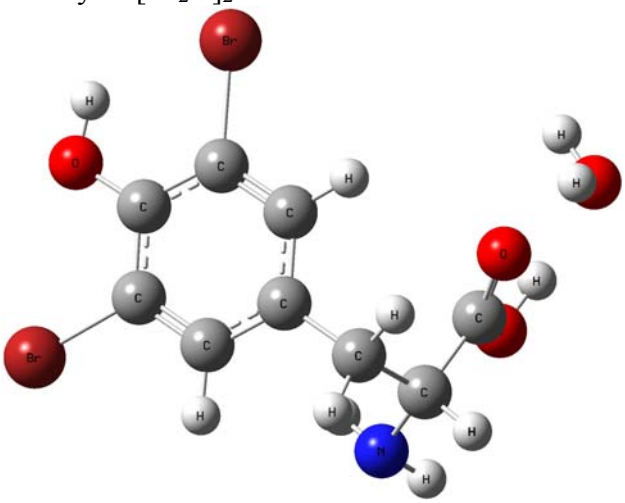

Figure S9. Optimized geometry of $[Br_2Y][H_2O]$.

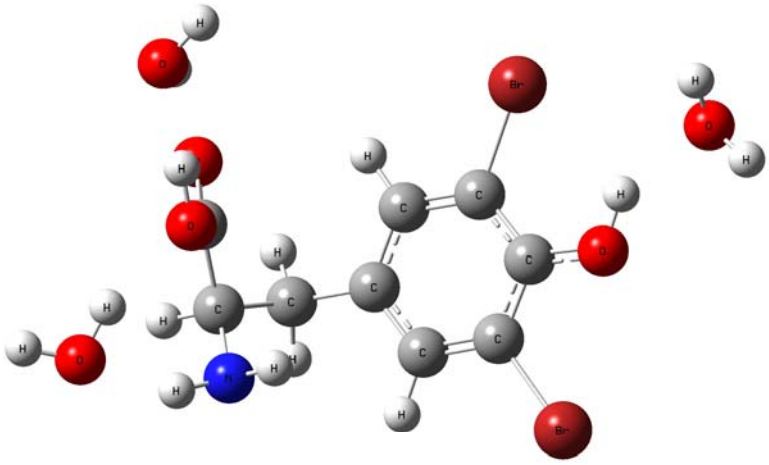

Figure S10. Optimized geometry of $[Br_2Y][H_2O]_3$.

S7. LDPI-MS of Br_2Y Films at Higher Photon Energies. See main text for discussion of this figure.

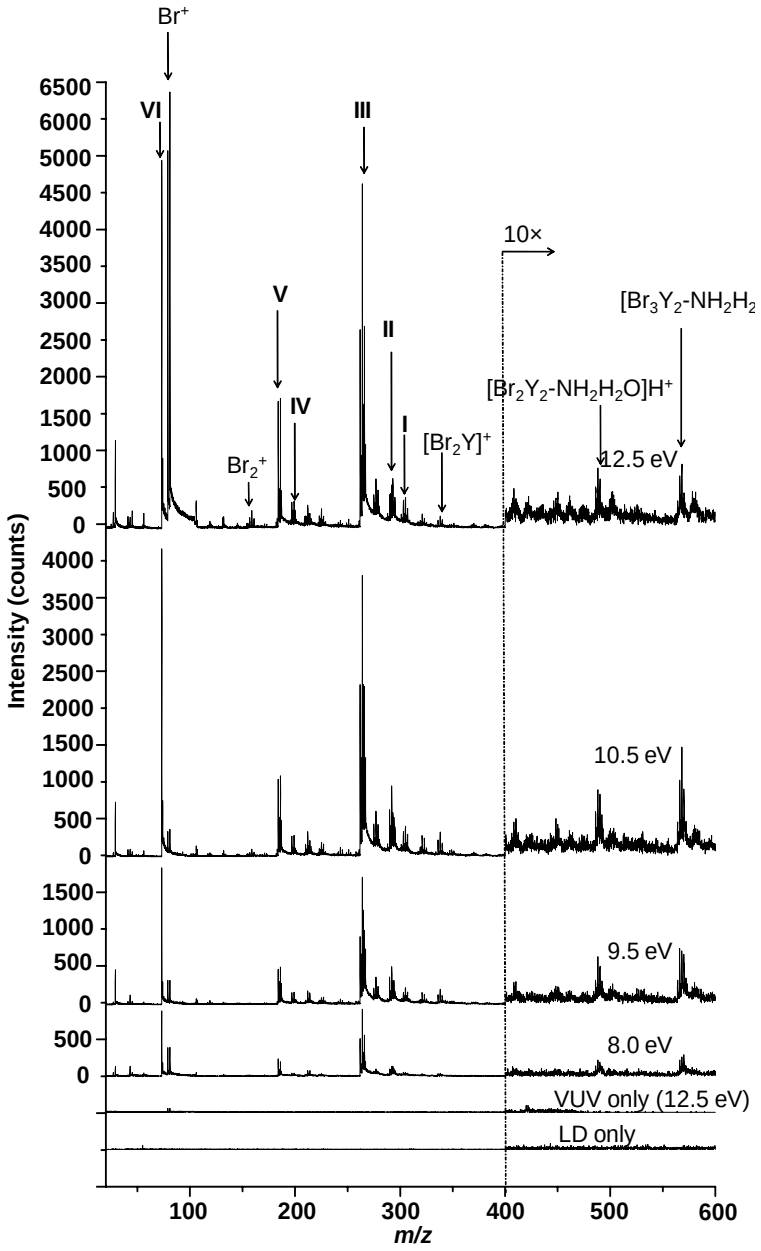

Figure S11. LDPI-MS of Br_2Y films recorded with 8.0 - 12.5 eV photon energies produced at the synchrotron. The "VUV only" spectrum was recorded with 12.5 eV photons, but without laser desorption while the "LD only" spectrum is recorded with the desorption laser but without any photoionization.

S8. Positive Ion SIMS of PEMs and Br_2Y-PEMs. Neat PEMs and Br_2Y-PEMs were also analyzed by 25 keV Bi_3^+ SIMS and the positive ion spectra are shown in Figure S12. Both spectra show several peaks that are characteristic to chitosan and alginate fragments: the peak at m/z 199.1 was attributed to the $[C_6H_8O_6Na]^+$ alginate monomer, m/z 125 to the $[C_3H_2O_4Na]^+$ alginate fragment, and m/z 97.2 to $[C_6H_9O]^+$ from both chitosan and alginate.[37,38] Higher mass (as yet unidentified) fragments were also observed at m/z 250.2 and m/z 275, with additional lower mass peak groups below m/z 100 resulting from extensive chitosan/alginate degradation. However, SIMS of the Br_2Y-PEMs showed no evidence for the presence of Br^+ in the multilayer, where the vertical lines in the inset indicate where $^{79}Br^+$ and $^{81}Br^+$ would appear. Even the Br^+ region did not display any signal unique to the Br_2Y-PEM. While the Br_2Y-PEM did show unique peaks at m/z 111.6 and 137.8, these lacked the characteristic isotopic distribution for bromine and therefore could not have resulted solely from any Br-containing fragments of Br_2Y.

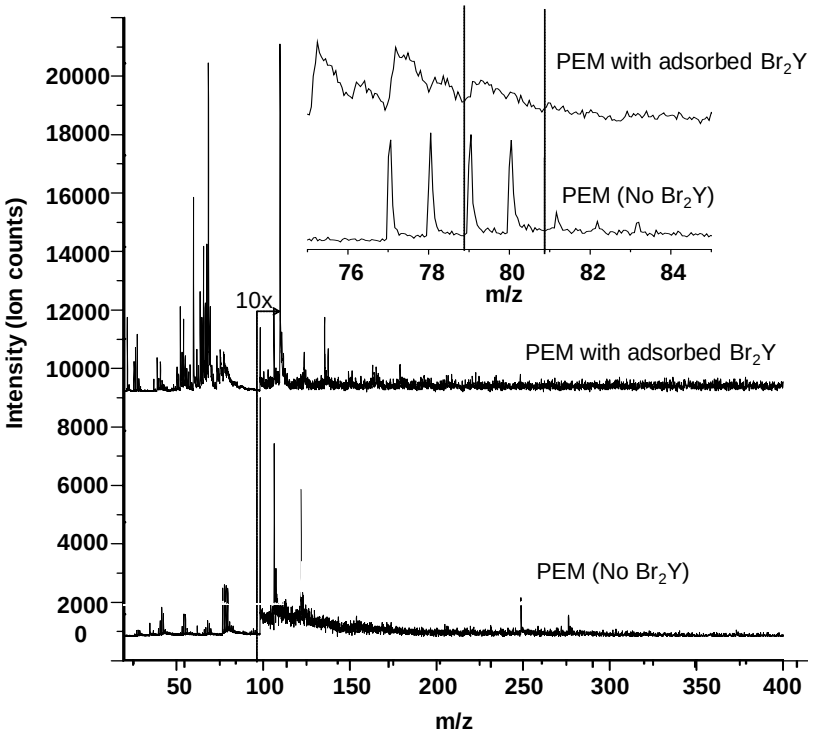

Figure S12. Positive ion 25 keV Bi_3^{2+} SIMS of PEM and Br_2Y-PEM. Vertical lines in inset indicate where $^{79}Br^+$ and $^{81}Br^+$ would appear.